



ORIGINAL ARTICLE

Sustainable synthesis of Cu NPs decorated on pectin modified Fe₃O₄ nanocomposite: Catalytic synthesis of 1-substituted-1*H*-tetrazoles and *in-vitro* studies on its cytotoxicity and anti-colorectal adenocarcinoma effects on HT-29 cell lines



Weisong Xue^{a,b}, Guohua Yang^{a,*}, Bikash Karmakar^c, Yi Gao^b

^a Department of General Surgery, The South Brother of Fujian Province Hospital, Fuzhou, Fujian Province 350000, China

^b General Surgery Center, Department of Hepatobiliary Surgery II, Guangdong Provincial Research Center for Artificial Organ and Tissue Engineering, Guangzhou Clinical Research and Transformation Center for Artificial Liver, Institute of Regenerative Medicine, Zhujiang Hospital, Southern Medical University, Guangzhou, Guangdong Province 510280, China

^c Department of Chemistry, Gobardanga Hindu College, 24 Parganas (North), India

Received 9 May 2021; accepted 30 June 2021

Available online 6 July 2021

KEYWORDS

Pectin;
Cu NP;
1-substituted tetrazoles;
Reusable;
Cytotoxicity;
Anti-colon cancer

Abstract A great deal of modern catalytic research orients around the architecturally designed bio-engineered catalysts. In this context, we have adorned Cu NPs over pectin encapsulated Fe₃O₄ NPs. The Cu NPs were generated following a biogenic green pathway over the core-shell type nanocomposite promoted by *Mentha Pulegium* flower extract as natural reducing/stabilizing agent. The as-synthesized nanocomposite was meticulously characterized by using a wide range of physicochemical techniques like FT-IR, FESEM, TEM, EDX, elemental mapping, VSM, XRD and ICP-OES analysis. The catalyst was explored in the synthesis of diversely substituted 1*H*-tetrazoles via three component coupling reaction (MCR), under solvent-less conditions affording high to excellent yields. Heterogeneity of the catalyst was measured through its excellent reusability, hot-filtration test and leaching study. The nanocomposite was also explored biologically in the anticancer assays. In the cytotoxicity and anti-human colon carcinoma studies, the nanocomposite was treated to colorectal adenocarcinoma (HT-29) cell line following MTT assay. The cell viability of malignant

* Corresponding author.

E-mail address: doctoryanguohua@sina.com (G. Yang).

Peer review under responsibility of King Saud University.



colon cell line reduced dose-dependently in the presence of Cu/Pectin@Fe₃O₄ nanocomposite. IC₅₀ values of the nanocomposite were observed to be 1450.84 µg/mL against HT-29 cell line. The outstanding results showed by the developed nanocomposite, could be highly promising in cancer management in near future.

© 2021 The Authors. Published by Elsevier B.V. on behalf of King Saud University. This is an open access article under the CC BY-NC-ND license (<http://creativecommons.org/licenses/by-nc-nd/4.0/>).

1. Introduction

In recent times, it has been a common trend to develop the functionalized nanomaterials in advanced level to improve their physicochemical, catalytic and biological properties. But, the advent of different efficient physical and chemical methods for the preparation of modified nanomaterials has concurrently upsetting the sustainability due to harshness of the protocol as well as the development of hazardous by-products. Hence, there is an obvious requirement for green technology in such processes (Gawande et al., 2013; Sadjadi et al., 2020). Consequently, ample research is being carried out on the bottom-up synthesis of materials involving functional biomolecules, more precisely, the phytochemicals derived from plant kingdom. Biogenetic architecture affords some unique features like uniform shape and tunable size in nano-dimensions, outstanding thermal and mechanical stability and large surface to volume ratio (Tamoradi et al., 2020b; Hemmati et al., 2020a; Tamoradi et al., 2020c; Veisi et al., 2019a; Veisi et al., 2020b; Tamoradi et al., 2021; Tamoradi et al., 2020a). The as-synthesized materials find enormous relevance in adsorption, degradation of dyes and contaminants, disposal of heavy and toxic metals, bio-sensing, drug delivery, biomedical applications and catalysis (Olivera et al., 2016; Awual et al., 2018; Mohammadi et al., 2020; Aguilera et al., 2019; Esmailpour et al., 2018; Lotfi and Veisi, 2019; Ding et al., 2015; Colombo et al., 2012; Cao et al., 2017). There has been tremendous significance of magnetic nanomaterials in these days owing to their excellent reusability and biocompatibility, facile synthesis, low toxicity, abundance and being very economical. In this regard, Fe₃O₄ nanoparticles (NP) have been come into prominence as an excellent support in the development of functionalized bio-nanomaterials. Moreover, the plentiful hydroxy groups over its surface facilitate the modification of outer layer that prevent the NPs from possible agglomeration, corrosion and unwanted oxidations (Gawande et al., 2013; Nasir Baig and Varma, 2013; Veisi et al., 2019b; Veisi et al., 2018a; Tamoradi et al., 2017; Veisi et al., 2018b; Farzad and Veisi, 2018). This has provoked us to employ the polysaccharide, pectin, a galacturonic acid copolymer, to shell the ferrite core, thereby shaping it a core-shell type nanocomposite (Pectin@Fe₃O₄). Finally, *in situ* synthesized Cu NPs have been fabricated over it with the aid of *Mentha Pulegium* flower extract as green reducing agent. It is anticipated that the biomolecules from the flower extract frames a network of polar organo-functions which anchors the Cu²⁺ ions and subsequently reduces them to Cu⁰ NPs (Hemmati et al., 2020b). In literature there have been several reports on the Cu NP-ferrite hybrid nanocomposite being used in broad range of applications including different types of organic transformations (Tamoradi et al., 2020b; Zarnegar and Safari, 2014; Pham et al., 2018; Zeynizadeh et al., 2020; Tang et al., 2014; Nasrollahzadeh et al., 2015; Moghaddam et al., 2021; Rezaei et al., 2018; Rahimi et al., 2020). We herein report the

biogenic synthesis of Cu/Pectin@Fe₃O₄ nanocomposite which has been further catalytically explored in the synthesis of 1-substituted-1*H*-tetrazoles following a three component coupling at solvent-less conditions.

Tetrazoles are high nitrogen containing heterocycles having plethora of applications in pharmaceuticals and drug designing, as explosives, in material science and coordination chemistry. They are frequently used as bioisosters of carboxylic acids (Neochoritis et al., 2019) and important precursors towards other bioactive heterocycles like triazoles, thiazoles and oxazolidones. In organic synthesis of tetrazoles, there are numerous reports on 5-substituted derivatives, but in comparison, that of 1-substituted tetrazoles are rather limited (Nasrollahzadeh et al., 2019). Our protocol involves the click chemistry for assembling diverse arylamines, triethyl orthoformate and sodium azide towards the synthesis of a library of 1-substituted-1*H*-tetrazoles over the Cu/Pectin@Fe₃O₄ nanocomposite, being hitherto unreported.

Furthermore, the material was investigated in different biological assays like study of antioxidant, cytotoxicity and anti-colon cancer properties. Colon or colorectal cancer (CRC) is one of the most invasive and prevalent cancer affecting the gastrointestinal system of human and the second leading cancer in terms of mortality in the world (Dong et al., 2019; Lin et al., 2020). The general indications for CRC are constipation, irregular or incomplete bowel movement, rectal bleeding, weakness, fatigue and abnormal weight loss. Surgery, chemotherapy, radiotherapy and targeted therapy are the conventional treatments procedures for CRC (Han et al., 2019; Valeri, 2019). However, owing to some serious side effects like swelling or bruising of the incision area, damage of nerves, toxicity, hair loss, fatigue, diarrhea etc, researchers have been persistently engaged to find out new formulations. In search of unconventional formulations, recently, metal nanoparticles (MNP) have come into prominence to put up with excellent anticancer properties without any adverse effects (Abdel-Fattah and Ali, 2018; Patil and Kim, 2017; Bisht and Rayamajhi, 2016; Hassanien et al., 2018). Several bio-engineered MNPs have been developed henceforth towards the high-end cancer research. This has persuaded us to engage the Cu/Pectin@Fe₃O₄ nanocomposite in the CRC *in vitro* studies.

2. Experimental

2.1. Materials and methods

A.R grade CuCl₂·2H₂O, FeCl₃, Pectin was purchased from Sigma-Aldrich. CH(OEt)₃, NaN₃, organic substrates and all the solvents were procured from Merck. MTT dye was purchased from Fluka. All the reagents were used without further purification. The solvents were used after distillation and dried over 4 Å molecular sieves. Structural morphology and elemental analysis was studied using a FESEM-TESCAN MIRA3

microscope equipped with EDX (TSCAN). The samples were gold coated prior to analysis in the instrument. For elemental analysis a section of the FESEM image was X-ray scanned to have the distribution of species. The FT-IR was done on KBr disc in a Bruker VERTEX 80 v spectrophotometer. TEM analysis was performed with a Philips CM10 microscope at an operating voltage of 200 Kv. The samples were prepared by adsorption of acetn dispersed sample on a carbon coated Cu grid. The powder XRD of the nanostructures were done using Co K α radiation ($\lambda = 1.78897 \text{ \AA}$) with operating at 40 keV, and a cathode current of 40 Ma in the scanning range of $2\theta = 5$ to 80° . VSM measurement was recorded in a vibrating sample 244 magnetometer MDKFD at room temperature. A STAT FAX 2100, BioTek, Winooski, USA instrument was used in Microplate Reading.

2.2. Aqueous extraction of *Mentha pulegium* flower

2.0 gm of fresh *Mentha pulegium* flower petals was dispersed over 100 mL DI water and stirred vigorously at 80°C for 20 min. Subsequently, the mixture was filtered over Whatman No. 1 paper to remove the undissolved plant residues. The colored filtrate was further centrifuged at 4000 rpm for 5 min and the clear supernatant layer was decanted off for further use.

2.3. Synthesis of the Pectin@Fe₃O₄ nanocomposite

Fe₃O₄ NPs were prepared through typical co-precipitation method as published earlier (Veisi et al., 2019b). 0.5 g of pectin was dissolved in 100 mL water by sonication for 20 min. Subsequently, 0.5 g of the Fe₃O₄ NPs were dispersed in the pectin solution and left stirred for 12 h at ambient conditions. The resulting nanocomposite (Pectin@Fe₃O₄) was isolated by magnetic decantation, washed thoroughly with DI water and dried in air.

2.4. Synthesis of Cu/Pectin@Fe₃O₄ nanocomposite

0.5 g Pectin@Fe₃O₄ was initially dispersed in the 100 mL flower extract with continuous stirring and then a solution of 0.1 g CuCl₂·2H₂O salt in minimum volume of DI water added dropwise to it. The mixture was then warmed at 80°C for 5 h. The precipitate so obtained was retrieved using an external magnet, washed with DI water and dried in air. ICP-OES analysis was used to assess the Cu content on the material and found to be 0.25 mmol/g.

2.5. General procedure for the catalyzed synthesis of 1-substituted-1H-tetrazoles

In a solvent-free mixture of amine (aromatic and aliphatic), NaN₃ and triethylorthoformate, taken in 1:1:1.2 mol ratio, 0.02 g the Cu/Pectin@Fe₃O₄ (0.5 mol%) catalyst was added and heated at 100°C for requisite times. After completion (by TLC), the reaction mixture was diluted with 10 mL EtOAc to separate the catalyst magnetically. Subsequently, the organic layer was washed with water and collected by solvent extraction. The collected organic fraction was dried, concentrated and simply recrystallized to have the pure product.

2.6. MTT assay protocol

The mentioned cell line was cultured in 1×10^5 cell/well in 96-well plates for 24 h at optimal conditions (37°C , 5% CO₂ in humidified incubator). Thereafter, the growth media (10% FBS) was removed and the cells were washed twice with PBS. In the new RPMI medium (10% FBS) 0.5, 5, 50, 500 and 1000 $\mu\text{g/mL}$ of the synthesized compounds was added and the cells were incubated for another 72 h. The triple wells were analyzed for each concentration and column elution buffer was used as the control. Then 10 μL solution of freshly prepared 5 mg/mL MTT dye in PBS was added to each well and allowed to incubate for an additional 4 h. The media was subsequently removed and DMSO was added at a concentration of 100 $\mu\text{L/well}$. Plates were shaken gently to facilitate formazan crystal solubilization. Finally, absorbance of each of the samples was measured at 545 nm using a microplate reader. The percentages of cell toxicity and half-maximal inhibitory concentration (IC₅₀) were calculated as the following

$$\text{Toxicity}\% = \left(1 - \frac{\text{mean OD of sample}}{\text{mean OD of control}}\right) \times 100$$

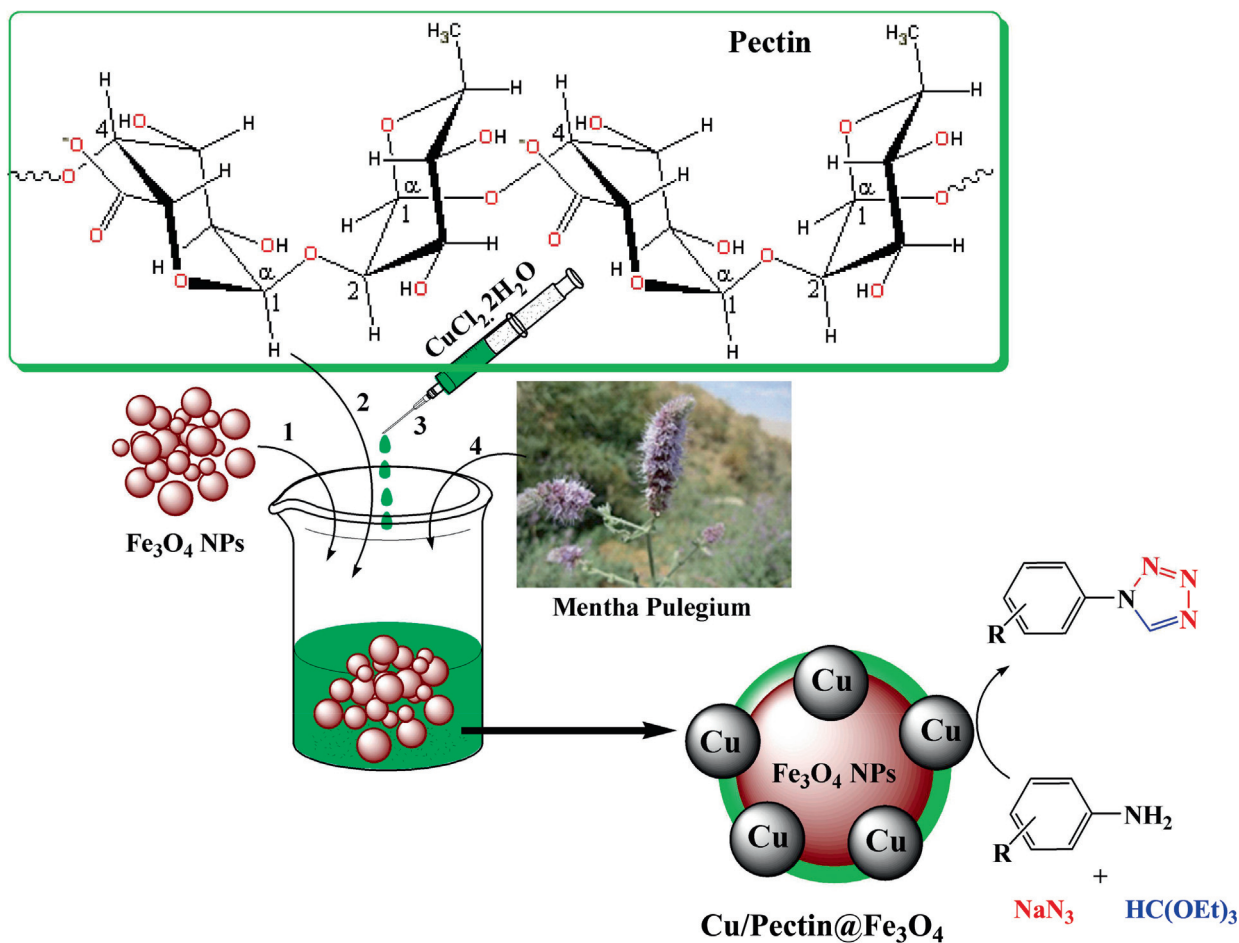
$$\text{Viability}\% = 100 - \text{Toxicity}\%$$

3. Results and discussion

3.1. Catalyst characterization data analysis

The biogenic Cu grafted and pectin modified ferrite core-shell type as synthesized nanocatalyst (Scheme 1) was physicochemically characterized over a diverse range of analytical methods like FE-SEM, TEM, EDX, FT-IR, VSM, elemental mapping, XRD and ICP-OES. Fig. 1 represents a comparative FT-IR spectrum of bare Fe₃O₄, pectin, pectin@Fe₃O₄ and Cu/Pectin@Fe₃O₄ in order to explain the stepwise architecture of the final material. Markedly, a characteristic strong absorption peak is observed at 582 cm^{-1} due to Fe–O–Fe stretching in the spectrum of Fe₃O₄ (Fig. 1a). The sharp peak at 1635 cm^{-1} refers to the H–O–H bending vibrations attributed to the water molecules present at its surface. Fig. 1b shows the featured peaks of pectin, namely, O–H bending, C–O stretching, C–O–C asymmetric stretching and C–C stretching, being appeared at 1652, 1382, 1158 and 1081 cm^{-1} respectively (Konda et al., 2014; Mazaahir et al., 2012). The FT-IR spectrum of pectin@Fe₃O₄ is evidently a composite of the earlier two peaks validating their successful assembling (Fig. 1c) only a slight shifting of peak positions. Finally, the Cu/Pectin@Fe₃O₄ material is depicted in Fig. 1d where all the other constituting peaks remained intact, except the peak intensity of O–H stretching vibrations at $\sim 3400 \text{ cm}^{-1}$ being slightly diminished, attributed to the strong interactions with Cu NPs (Veisi et al., 2020a; Veisi et al., 2021; Hemmati et al., 2021).

The inherent microstructural features, morphology, texture and shape of the as-synthesized Cu/Pectin@Fe₃O₄ nanocomposite were determined by SEM and TEM analysis. Fig. 2 representing the SEM image, depicts the globular morphology of the NPs having mean diameter of 30–40 nm. A thin uniform and continuous distribution of pectin over the core ferrite towards the surface functionalization can be anticipated from



Scheme 1 Schematic synthesis of Cu/Pectin@Fe₃O₄ nanocomposite and its application for one-pot synthesis of 1-substituted-1H-tetrazoles.

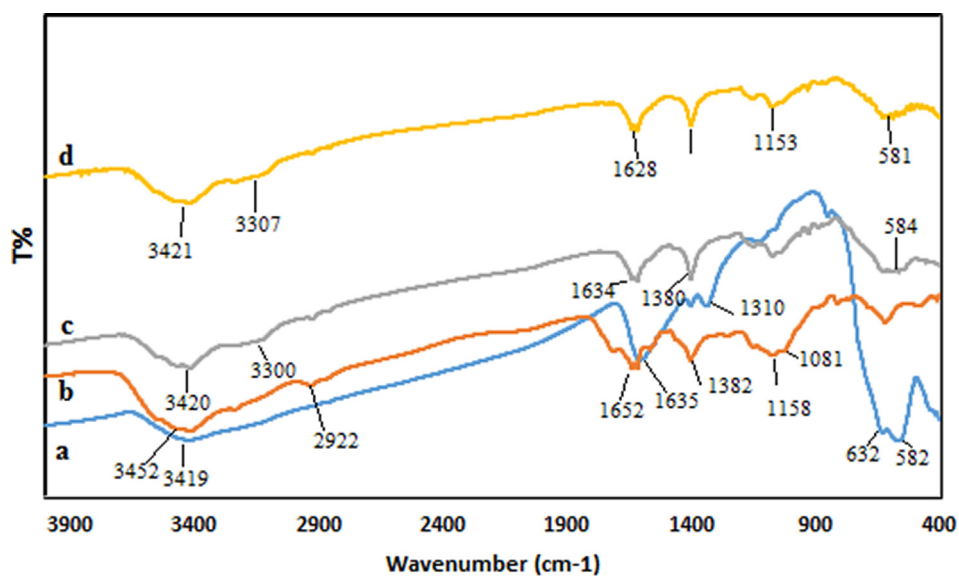


Fig. 1 FT-IR spectra of a) Fe₃O₄, b) Pectin, c) Pectin@Fe₃O₄, and d) Cu/Pectin@Fe₃O₄.

the appearances. However, the presence of Cu NPs could not be separately detected from the images. Owing to manual sam-

pling, the particles are somewhat aggregated, as can be seen from the image.

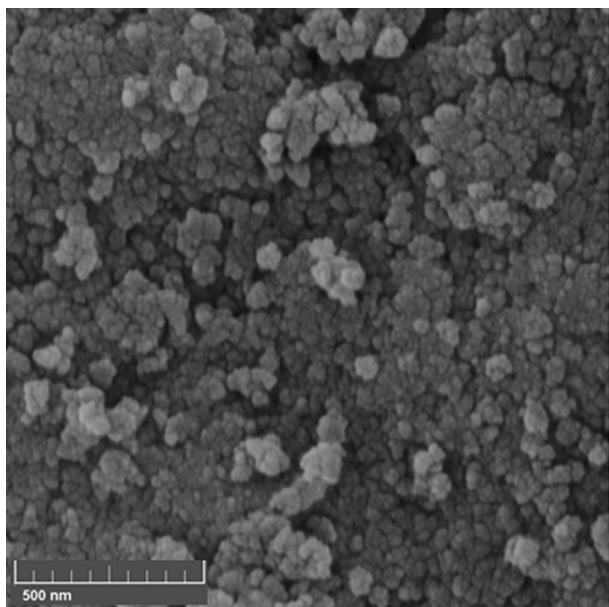


Fig. 2 FE-SEM image of Cu/Pectin@Fe₃O₄ nanocomposite.

Some more details of the structural inheritance were established through TEM analysis (Fig. 3). It clearly displays the fabrication of tiny spherical Cu NPs over the dark Pectin@Fe₃O₄ surface. The Cu NPs are attached via plant phytochemicals which also *in situ* stabilizes them by capping. The small Cu NPs at external surface are homomorphic and of ~20–40 nm in size.

In order to have an idea of chemical composition of the nanocomposite, EDX analysis was carried out and the profile is shown in Fig. 4. It represents Fe and Cu as metallic components. The occurrence of Cu confirmed the successful fabrication of Cu NP over the composite surface. Au peaks come by default as a result of Au coating on the sample prior to the EDX analysis. The presence of C and O are the evidence of biomolecular attachments. The results were further justified by FE-SEM elemental mapping analysis (Fig. 5). The compositional map reveals the Fe, C, and Cu species to exist with excellent dispersion throughout the matrix surface. Fine distribution of active species on the catalyst surface definitely has a significant impact on the catalytic performance.

Due to iron core based material, study of magnetism seems to an obvious measure. Fig. 6 reveals the magnetic hysteresis curves of the bare Fe₃O₄ and Cu/Pectin@Fe₃O₄. Against a variable external magnetic field both the materials show significant magnetic properties at room temperature and the nature of curves evidently says their paramagnetic character. The saturation magnetization values (M_s) of the materials were found to be 61.2 and 24.8 emu/g respectively. The decrease in magnetism in the modified material can be predicted from the incorporation of non-magnetic Cu (Zheng et al., 2020); *Mentha pulegium* extracts and pectin respectively over the magnetic core.

Crystalline phases and the diffraction planes of the said nanocomposite were ascertained by XRD study, being presented in Fig. 7. It represents a single phase profile indicating a united entity of the assembled counterparts. The typical diffraction peaks due to Fe₃O₄ are observed at $2\theta = 30.1, 35.6, 43.4, 53.7, 57.1, 62.9^\circ$ corresponding to (220), (311),

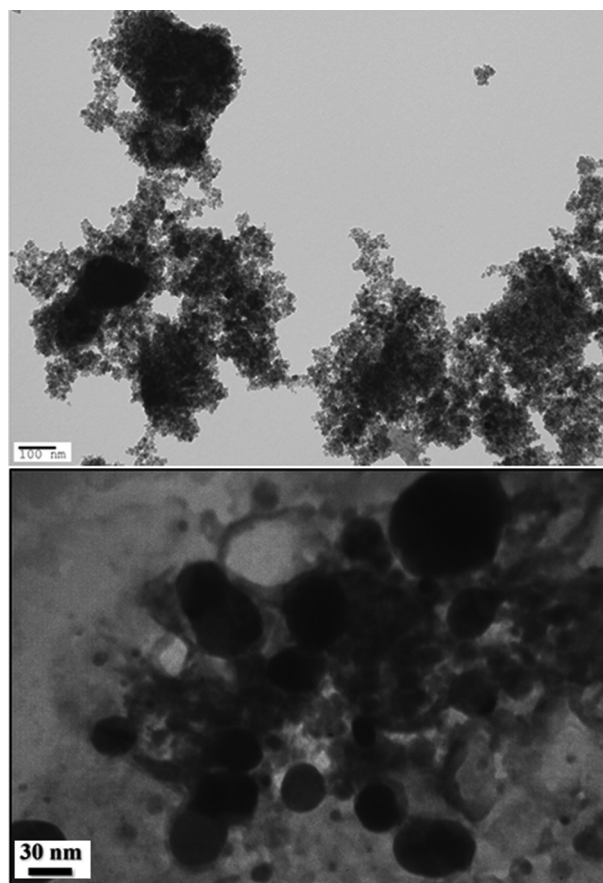


Fig. 3 TEM image of Cu/Pectin@Fe₃O₄ nanocomposite.

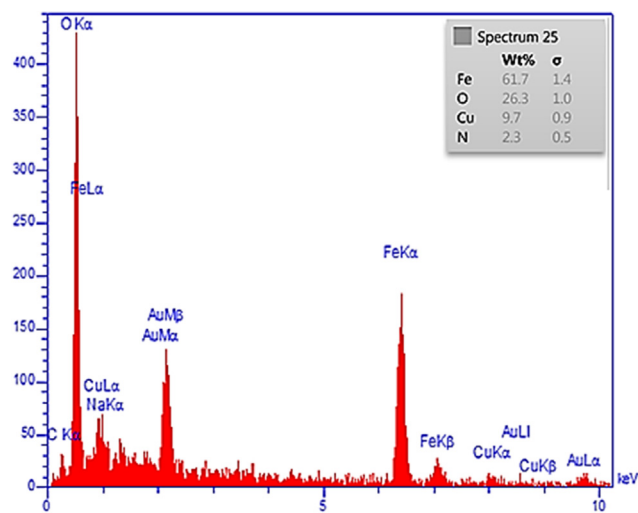


Fig. 4 EDX pattern of the nanocomposite.

(400), (422), (511) and (440) Bragg reflection planes respectively (JCPDS file, PDF No. 65-3107). Three additional sharp diffraction peaks observed at $2\theta = 43.1, 49.7$ and 75.4° are contributed from cubic crystalline Cu NPs being assigned to the (111), (200) and (220) diffraction planes, respectively

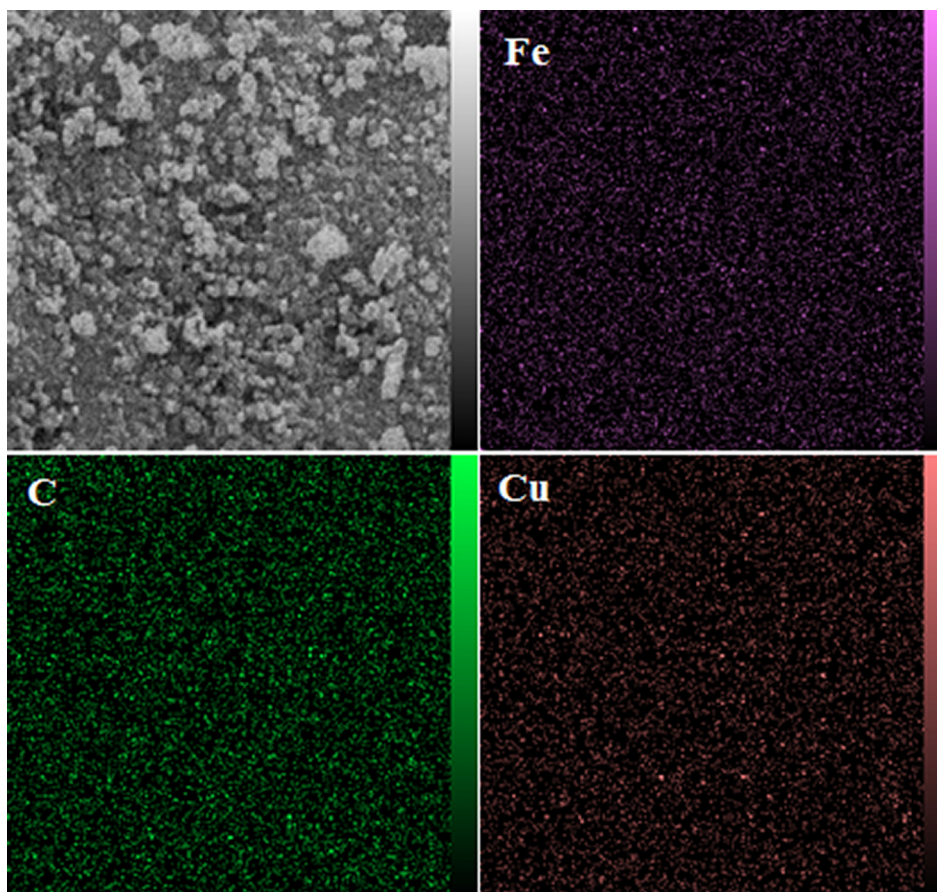


Fig. 5 Elemental mapping of Cu/Pectin@Fe₃O₄.

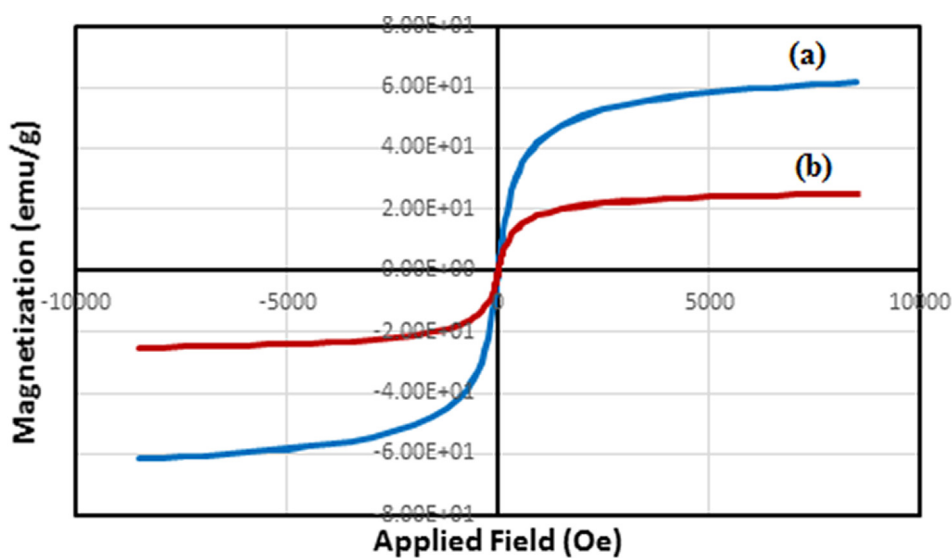


Fig. 6 Magnetic hysteresis curves of (a) Fe₃O₄ NPs, and (b) Cu/Pectin@Fe₃O₄.

which are in close agreement with the standard data (JCPDS No. 04-0784) (Joseph et al., 2016).

3.2. Catalytic applications and reaction data analysis

Just after the detailed microstructural study and analysis of physical properties, we headed towards the catalytic explo-

ration. Now, in an attempt to recognize the ideal catalytic conditions towards the tetrazole motif, the coupling of aniline, triethylorthoformate and sodium azide were initially chosen as a model reaction and an array of investigations were carried out using various parameters like solvent, catalyst load and temperature (Table 1). The optimization was started with screening of solvents over 0.5 mol% Cu/Pectin@Fe₃O₄

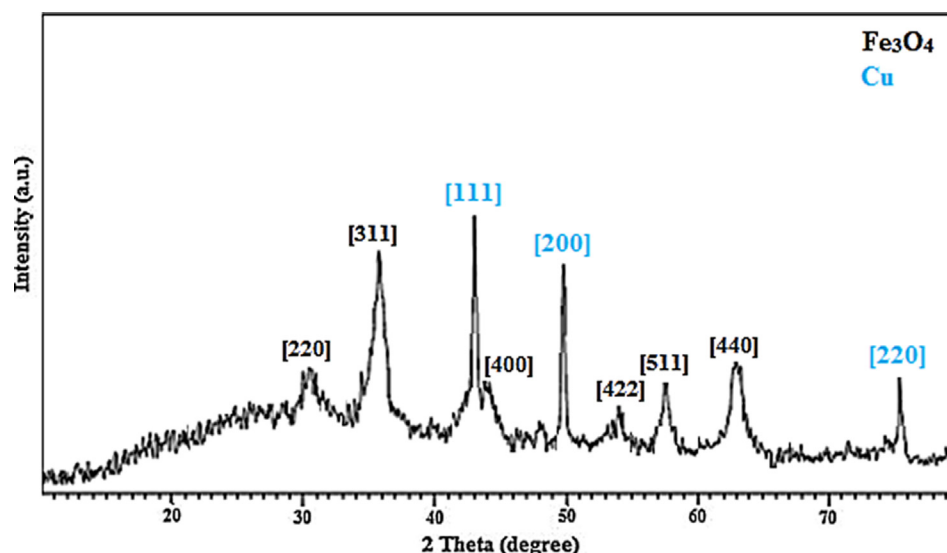


Fig. 7 XRD pattern of Cu/Pectin@Fe₃O₄.

Table 1 Optimization of reaction conditions for the synthesis of 1-phenyl-1H-tetrazoles.^a



Entry	Solvent	Catalyst (mol %)	Temp. (°C)	Time (h)	Yield (%) ^b
1	EtOH	Cu/Pectin@Fe ₃ O ₄ (0.5)	reflux	2	70
2	MeOH	Cu/Pectin@Fe ₃ O ₄ (0.5)	reflux	2	65
3	EtOH-H ₂ O	Cu/Pectin@Fe ₃ O ₄ (0.5)	reflux	2	60
4	DMF	Cu/Pectin@Fe ₃ O ₄ (0.5)	100 °C	2	80
5	CH ₂ Cl ₂	Cu/Pectin@Fe ₃ O ₄ (0.5)	reflux	2	40
6	CH ₃ CN	Cu/Pectin@Fe ₃ O ₄ (0.5)	reflux	2	50
7	H ₂ O	Cu/Pectin@Fe ₃ O ₄ (0.5)	reflux	2	10
8	toluene	Cu/Pectin@Fe ₃ O ₄ (0.5)	100 °C	2	60
9	Solvent-free	Cu/Pectin@Fe ₃ O ₄ (0.5)	100 °C	1	98
10	Solvent-free	Cu/Pectin@Fe ₃ O ₄ (0.5)	110 °C	1	98
11	Solvent-free	Cu/Pectin@Fe ₃ O ₄ (0.5)	80 °C	2	75
12	Solvent-free	Cu/Pectin@Fe ₃ O ₄ (0.6)	100 °C	1	98
13	Solvent-free	Cu/Pectin@Fe ₃ O ₄ (0.4)	100 °C	2	75
14	Solvent-free	Cu/Pectin@Fe ₃ O ₄ (0.3)	100 °C	2	60
15	Solvent-free	Cu/Pectin@Fe ₃ O ₄ (0.5)	25 °C	2	30
16	Solvent-free	None	100 °C	5	0
17	Solvent-free	Pectin (20 mg)	100 °C	5	10
18	Solvent-free	Fe ₃ O ₄ (20 mg)	100 °C	5	30
19	Solvent-free	Pectin@Fe ₃ O ₄ (20 mg)	100 °C	5	40
20	Solvent-free	Cu NPs	100 °C	2	95

^a Reaction conditions: aniline (1 mmol), triethylorthoformate (1.2 mmol) and sodium azide (1 mmol).

^b Isolated yield.

nanocatalyst at their respective refluxing temperatures which generated low to moderate yields (Table 1, entries 1–9). Evidently, solvent-free condition was found perfect for the desired transformation (Table 1, entry 9) and we decided to continue with that for the further experiments. While varying the catalyst load and reaction temperatures, we found that 0.5 mol% catalyst load at 100 °C worked the best affording 98% yields (Table 1, entry 9). The reaction was slow at ambient tempera-

ture. Again, at higher catalyst load there was no further improvement in the reaction. Notably, the reaction failed in the absence of any catalyst (Table 1, entry 16). Also, different catalyst components like pectin, bare Fe₃O₄ and Pectin@Fe₃O₄ could not promote the reaction sufficiently (Table 1, entry 17–19). In this context, bare Cu NPs were found to be highly productive (entry 20), but they have the tendency towards agglomeration and are not suitable for good reproducibility.

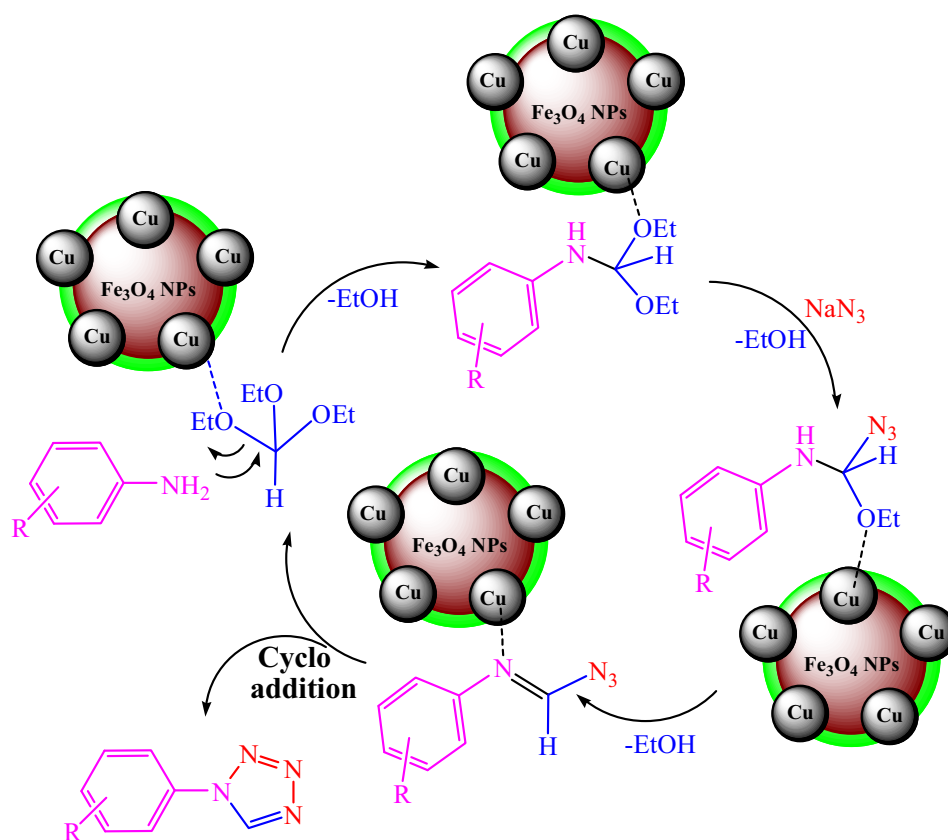
Table 2 Cu/Pectin@Fe₃O₄-Catalyzed synthesis of 1-substituted 1H-tetrazoles.^a

$$\text{R-NH}_2 + \text{HC(OEt)}_3 + \text{NaN}_3 \longrightarrow \text{R-N} \begin{array}{c} \diagup \text{N} \\ \diagdown \text{N} \\ \diagup \text{N} \\ \diagdown \text{N} \end{array}$$

Entry	R	Time (h)	Yield (%) ^b	Mp (°C)
1	C ₆ H ₅	1	98	61–62 (Dehghani et al., 2013)
2	4-Me-C ₆ H ₄	1	95	92–93 (Jin et al., 2008)
3	4-MeO-C ₆ H ₄	0.5	96	115–116 (Khalafi-Nezhad and Mohammadi, 2013)
4	4-Cl-C ₆ H ₄	1	96	151–152 (Khalafi-Nezhad and Mohammadi, 2013)
5	2,6-Cl ₂ -C ₆ H ₃	0.5	98	131–132 (Khalafi-Nezhad and Mohammadi, 2013)
6	4-NO ₂ -C ₆ H ₄	1.5	90	200–201 (Dehghani et al., 2013)
7	4-OH-C ₆ H ₄	1.5	85	164–165 (Jin et al., 2008)
8	4-Br-C ₆ H ₄	1.25	88	170–171 (Khalafi-Nezhad and Mohammadi, 2013)
9	C ₆ H ₅ CH ₂	1.5	90	132–133 (Esmailpour et al., 2014)
10	3-Pyridyl	1.5	85	77–78 (Dehghani et al., 2013)
11	Butanal	3	80	142–143 (Dehghani et al., 2013)
12	Cyclohexyl	2	85	170–171 (Khalafi-Nezhad and Mohammadi, 2013)

^a Reaction conditions : amine (1 mmol), NaN₃ (1 mmol), triethylorthoformate (1.2 mmol), Cu/Pectin@Fe₃O₄ (0.5 mol%), solvent-free, 100 °C.

^b Isolated yields.



Scheme 2 Proposed mechanism for the formation of 1-substituted-1H-tetrazoles catalyzed by Cu/Pectin@Fe₃O₄ nanocomposite.

In addition, isolation of them from the reaction mixture is quite tedious as compared to magnetic cored Cu NPs. Hence, the reaction was optimized in presence of 0.5 mol% Cu/Pectin@Fe₃O₄ catalyst under solvent-free conditions at 100 °C.

Subsequently, in order to have the scope and limitations of the optimized conditions for the synthesis of tetrazoles, a diverse range of amines were employed as variable substrate in the reaction along with CH(OEt)₃ and NaN₃. The outcomes are documented in Table 2. Aniline was converted to corre-

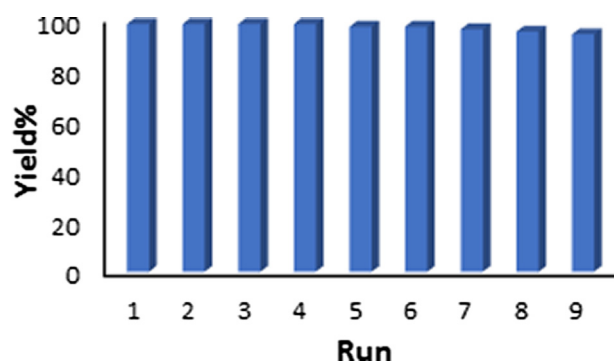


Fig. 8 Recyclability of Cu/Pectin@Fe₃O₄ nanocomposite in the synthesis of 1-phenyl-1H-tetrazole.

sponding tetrazole in just 1 h with 98% yield. The differently substituted arylamines were found to be highly compatible under the stabilized conditions. There was no significant difference in the electron releasing (Me, OMe) or withdrawing effect (Cl, Br, NO₂) in the yields. The reactions were equally successful irrespective of the geometrical position of substituents. Aliphatic amines reacted sluggishly over the aromatic amines (Table 2, entries 11, 12). Finally, the isolated pure products

were authenticated by comparing their corresponding melting points with literature.

3.3. Study of reaction mechanism

The plausible mechanistic pathway for the synthesis of 1-substituted-1H-tetrazoles following catalyzed click chemistry has been presented in Scheme 2. Initially, the amine reacts with catalyst activated triethyl orthoformate to form an amino acetal derivative. Then removal of EtOH produces an imino acetate intermediate *in situ*. Nucleophilic attack to this activated centre by azide ion and subsequent elimination of another molecule of EtOH affords an imino azide moiety. The final tetrazole molecule is obtained when this interesting intermediate undergoes an intramolecular [3 + 2] cycloaddition reaction initiated by Cu catalyst following 'click chemistry'. The catalyst this way relieves the product and gets free for being reused in another cycle (Kazemnejadi and Sardarian, 2016; Kazemnejadi et al., 2020; Xu et al., 2021).

3.4. Study of reusability and heterogeneity

In heterogeneous green catalysis, easy isolation and reusability of catalyst is considered as a fundamental criterion.

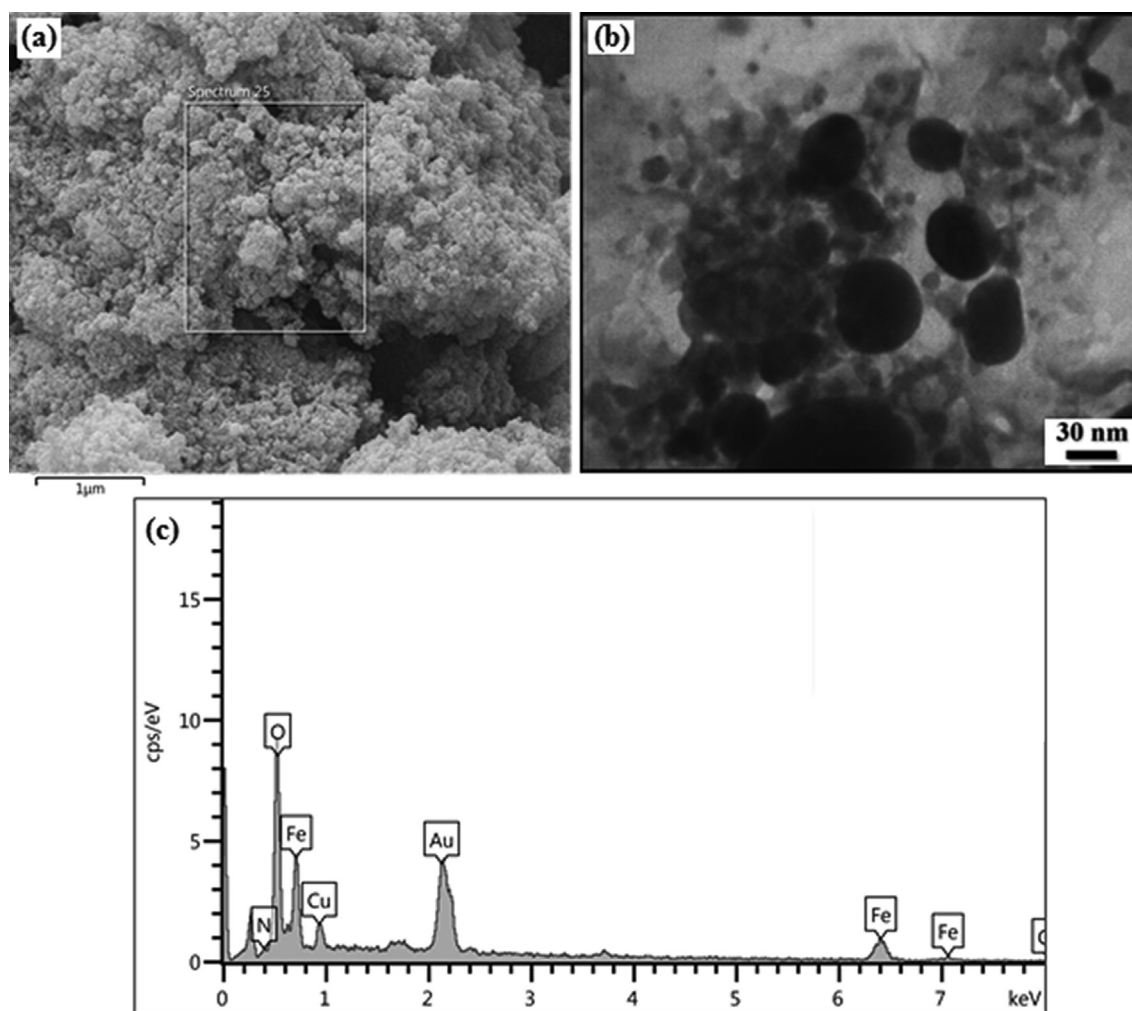


Fig. 9 (a) FESEM, (b) TEM and (c) EDX analysis of recycled Cu/Pectin@Fe₃O₄ catalyst after 9th run.

Consequently, after completion of a fresh catalyzed probe reaction, the catalyst was retrieved simply by using a magnet, washed thoroughly with EtOH and dried for reuse in further cycles. Interestingly, we got almost intact catalytic activity up to 9 consecutive cycles, as shown in Fig. 8. The FESEM, EDX and TEM analysis (Fig. 9) of the reused catalyst after 9th cycles confirmed the protection of the catalyst's nanostructure.

Again, in order to study the true heterogeneity of the Cu/Pectin@Fe₃O₄ nanocomposite and chances of leaching of Cu NPs, a hot filtration test was conducted with the model reaction. While running the fresh batch, the catalyst was isolated off at 30 min when it was of 60% yield and the catalyst-free reaction mixture was stirred for another 30 min keeping other conditions same. Incidentally, the reaction afforded no augmentation in its yield. This in turn also signifies that no active catalytic species was leached out of the nanocomposite and the catalyst could be considered as a true heterogeneous catalyst. The fact was justified by ICP-OES analysis of the reaction filtrate which revealed that very insignificant amount of Cu was leached out (0.01 wt% of the initial load) and that was catalytically inactive.

3.5. Cytotoxicity and anti-human colon cancer potentials of Cu/Pectin@Fe₃O₄ nanocomposite

While studying the cytotoxicity of Cu/Pectin@Fe₃O₄ along with Pectin@Fe₃O₄ and Fe₃O₄ on HT29 cells following MTT test, the cells were treated with several concentrations of the catalysts and observed for 48 h. The corresponding absorbances of the dye treated cells were measured at 545 nm. The Cu/Pectin@Fe₃O₄ nanocomposite exhibited an extraordinary viability on HT29 cell line even up to 2000 µg/mL of its concentration (Fig. 10). The results clearly showed that the cell viability got reduced dose-dependently in the presence of Cu/Pectin@Fe₃O₄. The IC₅₀ of Fe₃O₄, Pectin@Fe₃O₄ and Cu/Pectin@Fe₃O₄ nanocomposite were >2000, >2000, and 1450.84 µg/mL against HT29 cell line, respectively (Table 3).

In continue, the cell viability of HUVEC (normal cell line) under different concentration of Fe₃O₄ and Cu/Pectin@Fe₃O₄

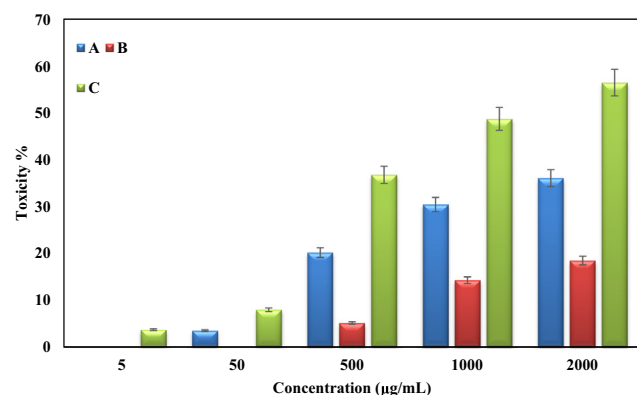


Fig. 10 The anti-human colon cancer properties (Cell viability (%)) of (a) Fe₃O₄, (b) Pectin@Fe₃O₄ and (c) Cu/Pectin@Fe₃O₄ nanocomposite (Concentrations of 0–2000 µg/mL) against HT29 cell line.

Table 3 The IC₅₀ of Fe₃O₄, Pectin@Fe₃O₄ and Cu/Pectin@Fe₃O₄ nanocomposite against HT29 cell line.

	Fe ₃ O ₄	Pectin@Fe ₃ O ₄	Cu/Pectin@Fe ₃ O ₄
IC ₅₀ (µg/mL)	>2000	>2000	1450.84

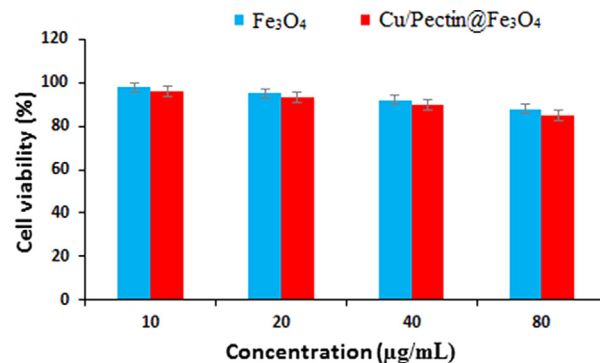


Fig. 11 In vitro cytotoxicity analysis of Fe₃O₄ and Cu/Pectin@Fe₃O₄ nanocomposite on HUVEC cell line.

nanocomposite were evaluated using the MTT method. As the results show (Fig. 11), Fe₃O₄ and Cu/Pectin@Fe₃O₄ nanocomposite do not significant effect on the viability of normal cells.

It is anticipated that the anti-human colon cancer effect of these nanoparticles is due to their very good antioxidant potentials. As the tumor progression is closely linked to inflammation and oxidative stress, a compound with good anti-inflammatory or antioxidant properties could have a potent anticarcinogenic property (Beheshtkhoo et al., 2018; Sangami and Manu, 2017).

4. Conclusion

In summary, we have developed a biogenic green method for the synthesis of tiny Cu NPs fabricated pectin functionalized ferrite NPs as an advanced nanocomposite material using *Mentha pulegium* flowers extract. The core-shell like environment in the pectin@Fe₃O₄ composite provides it rigidity. Moreover, the phytochemicals derived from the plant helps to anchor the incoming Cu ions first and subsequently reduces them exploiting the polar electron rich functional groups. The NPs generated at the outer layer also gets stabilized by them. Physicochemical features of the as-engineered material (Cu/pectin@Fe₃O₄) were assessed via several analytical methods. While exploring its catalytic activity we found it suitable in the three component coupling of various amines, triethylorthoformate and sodium azide towards a range of 1-substituted-1H-tetrazole derivatives. Under solvent-free conditions the reactions were highly productive. The role of Cu NP was inevitable as the bare pectin@Fe₃O₄ catalyst failed to make significant impact in the reaction. After the reaction the catalyst was retrieved easily by magnet and reused for nine times with consistent catalytic reactivity. There was also negligible leaching of Cu species in the reaction medium, justifying its true-heterogeneity. The nanocomposite was also explored biologically in the anticancer assays. In the cytotoxicity and anti-

human colon carcinoma studies, the nanocomposite was treated to colorectal adenocarcinoma (HT-29) cell line following MTT assay. The cell viability of malignant colon cell line reduced dose-dependently in the presence of Cu/Pectin@Fe₃O₄ nanocomposite. IC₅₀ values of the nanocomposite were observed to be 1450.84 µg/mL against HT-29 cell line. The promising results exhibited by the developed nanocomposite, could have a good potential as alternately formulation drug in cancer management.

5. Funding (Name of fund, subsidy number)

Science and Technnology Program of Fujian (2020GG0101002).

Declaration of Competing Interest

The authors declare that they have no known competing financial interests or personal relationships that could have appeared to influence the work reported in this paper.

References

- Abdel-Fattah, W.I., Ali, G.W., 2018. *J. Appl. Biotechnol. Bioeng.* 5 (2), 00116.
- Aguilera, G., Berry, C.C., West, R.M., Gonzalez-Monterrubio, E., Angulo-molina, A., Arias-Carrión, Ó., et al, 2019. *Nanoscale Adv.* 1, 671.
- Awual, M.R., Khraisheh, M., Alharthi, N.H., Luqman, M., Islam, A., Rezaul Karim, M., Rahman, M.M., Khaleque, M.A., 2018. *Chem. Eng. J.* 343, 118.
- Beheshtkhoo, N., Kouhbanani, M.A.J., Savardashtaki, A., et al, 2018. *Appl. Phys A* 124, 363.
- Bisht, G., Rayamajhi, S., 2016. *Nanobiomedicine* 3, 1.
- Cao, X., Tan, C., Sindoro, M., Zhang, H., 2017. *Chem. Soc. Rev.* 46, 2660.
- Colombo, M., Carregal-Romero, S., Casula, M.F., Gutiérrez, L., Morales, M.P., Böhm, I.B., Parak, W.J., 2012. *Chem. Soc. Rev.* 41, 4306.
- Dehghani, F., Sardarian, A.R., Esmaeilpour, M., 2013. *J. Organometal. Chem.* 743, 87.
- Ding, Y., Shen, S.Z., Sun, H., Sun, K., Liu, F., Qi, Y., Yan, J., 2015. *Mater. Sci. Eng. C* 48 (2015), 487.
- Dong, J., Li, J., Luo, J., Wu, W., 2019. *Eur. J. Inflamm.* 17, 1.
- Esmaeilpour, M., Javidi, J., Nowroozi Dodeji, F., Mokhtari Abarghoui, M., 2014. *J. Mol. Catal. A* 393, 18.
- Esmaeilpour, M., Sardarian, A.R., Firouzabadi, H., 2018. *J. Organometal. Chem.* 873, 22–34.
- Farzad, E., Veisi, H., 2018. *J. Indus. Eng. Chem.* 60, 114.
- Gawande, M.B., Branco, P.S., Varma, R.S., 2013. *Chem. Soc. Rev.* 42, 3371.
- Han, Y.D., Oh, T.J., Chung, T.H., 2019. *Clin. Epigenetics* 11, 51.
- Hassanien, R., Husein, D.Z., Al-Hakkani, M.F., 2018. *Heliyon* 12, e01077.
- Hemmati, S., Hekmati, M., Salamat, D., Yousefi, M., Karmakar, B., Veisi, H., 2020a. *Polyhedron* 179, 114359.
- Hemmati, S., Heravi, M.M., Karmakar, B., Veisi, H., 2020b. *J. Mol. Liq.* 319, 114302.
- Hemmati, S., Heravi, M.M., Karmakar, B., Veisi, H., 2021. *Sci. Rep.* 11, 12362.
- Jin, T., Kitahara, F., Kamijo, S., Yamamoto, Y., 2008. *Chem. Asian J.* 3, 1575.
- Joseph, A.T., Prakash, P., Narvi, S.S., 2016. *Int. J. Sci. Eng. Technol.* 4 (2), 463.
- Kazemnejadi, M., Mahmoudi, B., Sharafi, Z., Nasser, M.A., Allahresani, A., Esmaeilpour, M., 2020. *Appl. Organometal. Chem.* 34, (2) e5273.
- Kazemnejadi, M., Sardarian, A.R., 2016. *RSC Adv.* 6 (94), 91999.
- Khalafi-Nezhad, A., Mohammadi, S., 2013. *RSC Adv.* 3, 4362.
- Konda, S.R., Reguri, B.R., Kagga, M., 2014. *Der Pharma Chem.* 6, 228.
- Lin, A., Zhang, J., Luo, P., 2020. *Front. Immunol* 11, 2039.
- Lotfi, S., Veisi, H., 2019. *Mater. Sci. Eng. C* 105, 110112.
- Mazaahir, K., Ritika, C., Anwar, J., 2012. *Chin. Sci. Bull.* 57, 2273.
- Moghaddam, H.-R., Jamal, M.R.-N., Tajbaksh, M., 2021. *Sci. Rep.* 11, 2073.
- Mohammadi, P., Heravi, M.M., Sadjadi, S., 2020. *Sci. Rep.* 10, 6579.
- Nasir Baig, R.B., Varma, R.S., 2013. *Chem. Commun.* 49, 752.
- Nasrollahzadeh, M., Atarod, M., Sajadi, S.M., 2015. *Appl. Surf. Sci.* 364, 636.
- Nasrollahzadeh, M., Sajjadi, M., Tahsili, M.R., Shokouhimehr, M., Varma, R.S., 2019. *ACS Omega* 4, 8985.
- Neochoritis, C.G., Zhao, T., Dömling, A., 2019. *Chem. Rev.* 119, 1970.
- Olivera, S., Muralidhara, H.B., Venkatesh, K., Guna, V.K., Gopalakrishna, K., Kumar, Y., 2016. *Carbohydr. Polym.* 153, 600.
- Patil, M.P., Kim, G.-D., 2017. *Appl. Microbiol. Biotechnol.* 101, 79.
- Pham, V.L., Kim, D.-G., Ko, S.-O., 2018. *Chemosphere* 191, 639.
- Rahimi, J., Niksefat, M., Maleki, A., 2020. *Front. Chem.* 8, 1.
- Rezaei, M., Azizi, K., Amani, K., 2018. *Appl. Organometal. Chem.* 32, e4120.
- Sadjadi, S., Mohammadi, P., Heravi, M.M., 2020. *Sci. Rep.* 10, 6535.
- Sangami, S., Manu, M., 2017. *Environ. Technol. Innov.* 8, 150.
- Tamoradi, T., Choghamarani, A.G., Ghadermazi, M., 2017. *New J. Chem.* 41, 11714.
- Tamoradi, T., Karmakar, B., Kamalzare, M., Bayat, M., Kal-Koshvandi, A.T., Maleki, A., 2020a. *J. Mol. Struct.* 129, 128598.
- Tamoradi, T., Veisi, H., Karmakar, B., Gholami, J., 2020b. *Mater. Sci. Eng. C* 107, 110260.
- Tamoradi, T., Daraie, M., Heravi, M.M., Karmakar, B., 2020c. *New J. Chem.* 44, 11049.
- Tamoradi, T., Mousavi, S.M., Karmakar, B., 2021. *J. Iran. Chem. Soc.* <https://doi.org/10.1007/s13738-021-02241-9>.
- Tang, M., Zhang, S., Li, X., Pang, X., 2014. *Mater. Chem. Phys.* 148, 639.
- Valeri, N., 2019. *Cancer Res.* 79, 1041–1043.
- Veisi, H., Pirhayati, M., Kakanejadifard, A., Mohammadi, P., Abdi, M.R., Gholami, J., Hemmati, S., 2018a. *Chem. Select.* 3, 1820.
- Veisi, H., Hemmati, S., Safarimehr, P., 2018b. *J. Catal.* 365, 204.
- Veisi, H., Tamoradi, T., Karmakar, B., Mohammadi, P., Hemmati, S., 2019a. *Mater. Sci. Eng. C* 104, 109919.
- Veisi, H., Ghorbani, M., Hemmati, S., 2019b. *Mater. Sci. Eng. C* 98, 584.
- Veisi, H., Ozturk, T., Karmakar, B., Tamoradi, T., Hemmati, S., 2020a. *Carbohydr. Polym.* 225, 115966.
- Veisi, H., Tamoradi, T., Karmakar, B., Hemmati, S., 2020b. *J. Phys. Chem. Solids* 138, 109256.
- Veisi, H., Joshani, Z., Karmakar, B., Heravi, M.M., Gholami, J., 2021. *Int. J. Biol. Macromol.* 172, 104.
- Xu, D.P., Xiong, M., Kazemnejadi, M., 2021. *RSC Adv.* 11 (21), 12484.
- Zarnegar, Z., Safari, J., 2014. *New J. Chem.* 38, 4555.
- Zeynizadeh, B., Rahmani, S., Tizhoush, H., 2020. *Polyhedron* 175, 11420.
- Zheng, H., Huang, J., Zhou, T., Jiang, Y., Jiang, Y., Gao, M., Liu, Y., 2020. *Catalysts* 10, 1437.